JOURNAL OF APPLIED ELECTROCHEMISTRY 17 (1987) 347–356

Anodic characteristics of amorphous nickel-value metal alloys containing small amounts of platinum group elements in 0.5 M NaCl

N. KUMAGAI, Y. SAMATA

Daiki Engineering Co., Ltd, Shintoyofuta, Kashiwa 277, Japan

A. KAWASHIMA, K. ASAMI, K. HASHIMOTO

The Research Institute for Iron, Steel and Other Metals, Tohoku University, Sendai 980, Japan

Received 13 February 1986; revised 22 March 1986

By utilizing the characteristics of amorphous alloys capable of possessing specific electrocatalytic activity and corrosion resistance by alloying and surface activation treatment, an attempt was made to find amorphous alloys which are active as the anode material for production of sodium hypochlorite by electrolysis of seawater. Amorphous Ni–Nb and Ni–Ta alloys containing only 0.5–2.0 at % palladium and other platinum group metals showed a very high activity for chlorine production by electrolysis of 0.5 M NaCl at 30° C when they were previously immersed in 46% HF for surface activation. The current efficiency of these surface-activated alloys for chlorine evolution considerably exceeded that of the currently used, most active Pt–Ir/Ti electrode for electrolysis of seawater. The surface activation treatment resulted in preferential dissolution of alloy constituents unnecessary for the electrocatalytic activity, i.e. nickel and valve metals, with a consequent enrichment of electrocatalytically active platinum group elements in the surface-activated layer. The corrosion weight loss of the surface-activated amorphous alloys under the steady state conditions for chlorine production was undetectable by a microbalance.

1. Introduction

Since melt-spun amorphous Fe–Cr–P–C alloys with extraordinarily high corrosion resistances were discovered [1], a variety of unusual, unique and attractive chemical properties have been found [2]. The amorphous alloys consist of single-phase, solid solutions and are suitable for use in preparing materials of complicated compositions with specific properties by alloying with many different elements, even if the alloys of the same compositions that solidified without rapid quenching are composed of crystalline multiple phases and have poor mechanical properties (low strength and sometimes brittleness).

An anode for the electrolysis of sodium chloride solutions needs to have a high electrocatalytic activity for chlorine evolution and a low activity for parasitic oxygen evolution, along with a high corrosion resistance against extremely aggressive and highly oxidizing environments containing nascent chlorine. According to some of the present authors [3–7], some amorphous palladium base alloys possess very high corrosion resistance and electrocatalytic activity for the production of chlorine by the electrolysis of hot concentrated sodium chloride solutions. In these studies alloying and vitrification have been carried out to improve the corrosion resistance of rapidly corroding palladium in order to utilize the superior electrochemical properties of palladium, which has the highest electrocatalytic activity among the platinum group metals for chlorine evolution in sodium chloride solutions and a very low activity for parasitic oxygen evolution.

On the other hand, in industrial plants using

0021-891X/87 $03.00 + .12

seawater as a coolant, sodium hypochlorite is injected into the coolant at the intake of the cooling system for protection against marine life such as barnacles which decrease the cooling efficiency and sometimes clog the system. Sodium hypochlorite is produced by the reaction of chlorine with sodium hydroxide, both of which are products of the electrolysis of seawater at the anode and cathode, respectively. Accordingly, sodium hypochlorite is produced by the electrolysis of seawater without separation of anode and cathode compartments. It is necessary for anode materials for the production of sodium hypochlorite to have a much higher activity for chlorine evolution in comparison with the anode for chlorine evolution in hot concentrated sodium chloride solutions. This is because the concentration of chloride ion in seawater is almost one-eighth as high as the solutions used in the chlor-alkali industry, and because in the electrolysis of neutral seawater the oxygen evolution occurs at lower potentials than in acidic solutions; in addition, electrolysis occurs at ambient temperature.

Amorphous palladium-base alloys suitable as anode materials for the electrolysis of hot concentrated sodium chloride solutions are able to electrolyse seawater, and hence the enhancement of their activity has been attempted [8, 9] by applying a surface activation treatment consisting of (a) electrodeposition of zinc on the amorphous alloy, (b) heat treatment at lower temperatures than the crystallization temperature of the amorphous alloy for diffusion of zinc into the amorphous alloy, and (c) leaching of zinc from the alloy into a hot concentrated alkaline solution [10, 11]. Some of the surface-activated, amorphous, palladium-base alloys have been found to give current efficiencies greater than 90% for chlorine production in a 0.5 M NaCl solution at 30° C. This efficiency is much higher than the current efficiency of the Pt–Ir/Ti electrode ($\approx 80\%$), which is known to have the highest activity among currently used electrodes for the production of sodium hypochlorite by the electrolysis of seawater.

Because a high electric resistance along the longitudinal direction of the ribbon-shaped, thin amorphous alloys (several tens of micrometres thick) is unsuitable for utilization as the anode, the electrocatalytically active amorphous palladium-base alloys have been laser-processed as a surface layer on conventional crystalline bulk metals which would act as an electric conductor [12]. The electrochemical behaviour of the surface-activated amorphous surface alloy on a conventional crystalline nickel metal substrate has been investigated [13].

However, these alloys are composed mainly of platinum group metals, and other electrochemically active materials consisting of inexpensive elements are still required. The present work utilizes the characteristics of amorphous alloys capable of forming supersaturated, single-phase solid solutions containing various amounts of different elements, and aims to prepare amorphous alloys having a very high electrocatalytic activity for chlorine production in a dilute sodium chloride solution despite a very low concentration of electrocatalytically active platinum group metals.

2. Experimental details

A variety of nickel-base alloy ingots were cast by induction melting of commercial metals and home-made nickel phosphide under an argon atmosphere. After the ingot was remelted under an argon atmosphere in a quartz tube having a slit at the bottom, a jet of the molten alloy was impinged through the slit by pressurized argon gas onto the outer surface of a rapidly rotating wheel under an argon atmosphere. By this method amorphous alloy ribbons of 1–5 mm width and 10–30 μm thickness were prepared. The nominal compositions of the alloys are given in Tables 1 and 2. Prior to electrochemical measurements the amorphous alloy ribbons were polished in cyclohexane with silicon carbide paper up to No. 1000, degreased ultrasonically in acetone and dried in air. Enhancement of electrocatalytic activity was achieved by a surface activation treatment which is described later in this paper.

The electrolyte used was a 0.5 M NaCl solution open to air at 30 $\pm$ 1° C. Anodic polarization curves of specimens were measured potentiodynamically with a potential sweep rate of 2.6 ks V^{-1} without separation of the anode and cathode compartments. A platinum gauze and a saturated

Table 1. Nominal compositions of amorphous Ni–Ti, Ni–Zr and Ni–Nb alloys (at %)

Alloy	*Ni*	*Ti*	*Zr*	*Nb*	*Rh*	*Pd*	*Ir*	*P*
Ni–40Ti	60	40	0	0	0	0	0	0
Ni–40Zr	60	0	40	0	0	0	0	0
Ni–40Nb	60	0	0	40	0	0	0	0
Ni–40Nb–Rh	58	0	0	40	2	0	0	0
Ni–40Nb–Pd	59.95	0	0	40	0	0.05	0	0
	59.9	0	0	40	0	0.1	0	0
	59.7	0	0	40	0	0.3	0	0
	59.5	0	0	40	0	0.5	0	0
	59	0	0	40	0	1	0	0
	58	0	0	40	0	2	0	0
	57	0	0	40	0	3	0	0
Ni–40Nb–Pd–Ir	58.5	0	0	40	0	1	0.5	0
	58	0	0	40	0	1	1	0
Ni–40Nb–Ir	59.95	0	0	40	0	0	0.05	0
	59.9	0	0	40	0	0	0.1	0
	59.7	0	0	40	0	0	0.3	0
	59.5	0	0	40	0	0	0.5	0
	59	0	0	40	0	0	1	0
	58	0	0	40	0	0	2	0
Ni–50Nb–Ir	48	0	0	50	0	0	2	0
Ni–40Nb–Pd–P	57.9	0	0	40	0	0.1	0	2
	57.5	0	0	40	0	0.5	0	2
	57	0	0	40	0	1	0	2
	55	0	0	40	0	3	0	2

calomel electrode (SCE) were used as counter and reference electrodes, respectively. The ohmic drop in the potentiodynamic polarization measurements was corrected by estimation from the ohmic drop measured by the current interrupter method under galvanostatic conditions.

Galvanostatic polarization was performed at 500–5000 A m^{-2} in the 0.5 M NaCl solution at 30 $\pm$ 1° C and with a ratio of the solution volume to the specimen surface area of 30 to 400 cm in order to determine the current efficiency for the chlorine evolution on alloys at 1000 C l^{-1}. Because the anode and cathode compartments were not separated from each other, most of the chlorine formed on the anode seemed to react with sodium hydroxide formed on the cathode with a consequent formation of sodium hypochlorite. Both chlorine and sodium hypochlorite liberate iodine from potassium iodide. Accordingly, after the electrolysis an excess amount of potassium iodide was added to the electrolyte, and the amount of chlorine produced was estimated by iodometry by titration with a N/40 $Na_2S_2O_3$ solution.

An estimation of the corrosion rate under steady-state conditions for chlorine production was attempted as follows. The specimen was potentiostatically polarized at 1.25 V (versus SCE) for 12 h, rinsed with distilled water and acetone, and dried in a desiccator for 12 h. The specimen was then weighed by a microbalance. After the specimen had again been potentiostatically polarized at 1.25 V (SCE) for 24 h, the specimen was similarly rinsed and dried. The specimen was reweighed and the corrosion weight loss was estimated.

The surface-activated specimens were observed by means of a JEOL JSM-U3 scanning electron microscope, and the surface composition was examined by means of a dispersive X-ray spectrometer attached to the scanning electron microscope by a pentaerythritol crystal (PET).

3. Results and discussion

3.1. *As-cast amorphous alloys*

Fig. 1 shows polarization curves of amorphous

Table 2. Nominal compositions of amorphous Ni–30Ta alloys (at %)

Alloy	*Ni*	*Ta*	*Nb*	*Ru*	*Rh*	*Pd*	*Ir*	*Pt*	*Cu*	*Au*	*P*
Ni–30Ta–Ru	69	30	0	1	0	0	0	0	0	0	0
Ni–30Ta–Rh	69.5	30	0	0	0.5	0	0	0	0	0	0
	68	30	0	0	2	0	0	0	0	0	0
	67	30	0	0	3	0	0	0	0	0	0
	65	30	0	0	5	0	0	0	0	0	0
Ni–30Ta–Pd	69	30	0	0	0	1	0	0	0	0	0
	67	30	0	0	0	3	0	0	0	0	0
	65	30	0	0	0	5	0	0	0	0	0
	60	30	0	0	0	10	0	0	0	0	0
	50	30	0	0	0	20	0	0	0	0	0
Ni–30Ta–Ir	69.9	30	0	0	0	0	0.1	0	0	0	0
	69.5	30	0	0	0	0	0.5	0	0	0	0
	69	30	0	0	0	0	1	0	0	0	0
	68	30	0	0	0	0	2	0	0	0	0
	67	30	0	0	0	0	3	0	0	0	0
	60	30	0	0	0	0	10	0	0	0	0
Ni–30Ta–Pt	69	30	0	0	0	0	0	1	0	0	0
	67	30	0	0	0	0	0	3	0	0	0
Ni–30Ta–Rh–Pd	68.5	30	0	0	0.5	1	0	0	0	0	0
	66.5	30	0	0	0.5	3	0	0	0	0	0
	64.5	30	0	0	0.5	5	0	0	0	0	0
	59	30	0	0	1	10	0	0	0	0	0
Ni–30Ta–Ir–Pd	68.5	30	0	0	0	1	0.5	0	0	0	0
	66.5	30	0	0	0	3	0.5	0	0	0	0
	64.5	30	0	0	0	5	0.5	0	0	0	0
Ni–30Ta–Pd–P	67	30	0	0	0	1	0	0	0	0	2
	65	30	0	0	0	3	0	0	0	0	2
Ni–30Ta–Cu	69	30	0	0	0	0	0	0	1	0	0
Ni–30Ta–Au	69	30	0	0	0	0	0	0	0	1	0
	68	30	0	0	0	0	0	0	0	2	0

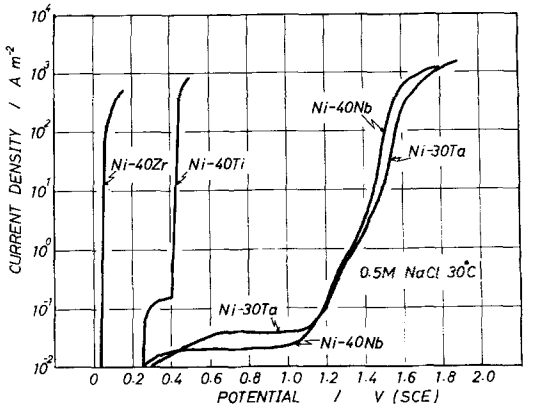

Fig. 1. Anodic polarization curves of amorphous binary nickel-valve metal alloys measured in 0.5 M NaCl at 30° C.

binary nickel alloys containing titanium, zirconium, niobium or tantalum measured in a 0.5 M NaCl solution in order to examine the corrosion resistance of alloys as an anode for the electrolysis of seawater. Since the pitting potential of amorphous Ni–40Ti and Ni–40Zr alloys are very low, they easily suffer pitting corrosion by anodic polarization at low potentials. In contrast, amorphous Ni–40Nb and Ni–30Ta alloys are spontaneously passive and are immune to pitting corrosion. The rise in current at high potentials is due to chlorine and oxygen evolution on the Ni–40Nb and Ni–30Ta alloys.

Since the niobium-containing or tantalum-containing alloys have sufficient corrosion

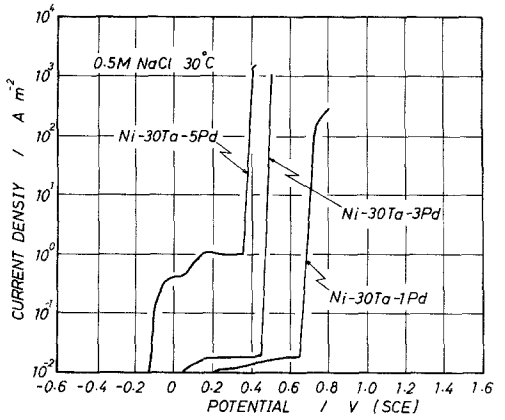

Fig. 2. Anodic polarization curves of amorphous Ni–30Ta–Pd alloys measured in 0.5 M NaCl at 30° C.

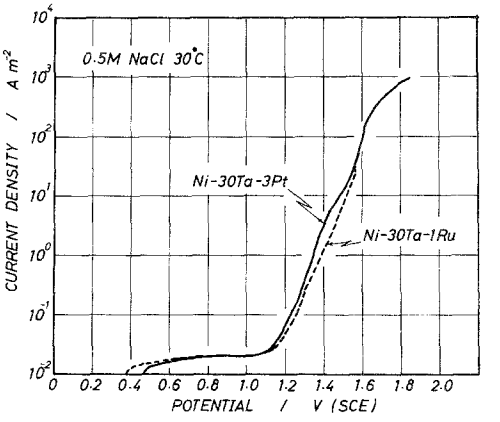

Fig. 4. Anodic polarization curves of amorphous Ni–30Ta–3Pt and Ni–30Ta–1Ru alloys measured in 0.5 M NaCl at 30° C.

resistance, an enhancement of their electrocatalytic activity was attempted by additions of small amounts of platinum group elements. It has been shown [4] that among platinum group metals palladium has the highest activity for chlorine evolution and a low activity for oxygen evolution in sodium chloride solutions at ambient temperature. Fig. 2 shows the change in the anodic polarization curves with the addition of palladium to the amorphous Ni–30Ta alloy. The addition of palladium leads to a sudden increase in current density by anodic polarization due to pitting corrosion. The pitting potential is lowered with increasing palladium content, indicating the detrimental effect of the palladium addition.

Palladium addition does not strongly influence the corrosion resistance of the amorphous Ni–40Nb alloy. As shown in Fig. 3, amorphous Ni–40Nb alloys containing 1–3 at % palladium are immune to pitting corrosion in the high potential region for chlorine production, although an excess addition of palladium such as 20 at % results in a sharp current increase at a potential as low as 0.4 V (versus SCE) owing to passivity breakdown.

Additions of small amounts of other platinum group elements are not detrimental to the passivity of amorphous Ni–30Ta and Ni–40Nb alloys as shown in Figs 4–6. Fig. 7 shows that the passivity of the amorphous Ni–30Ta alloy is not impaired by the addition of 1 at % gold but is broken at 0.8 V (versus SCE) by the addition of 2 at % gold.

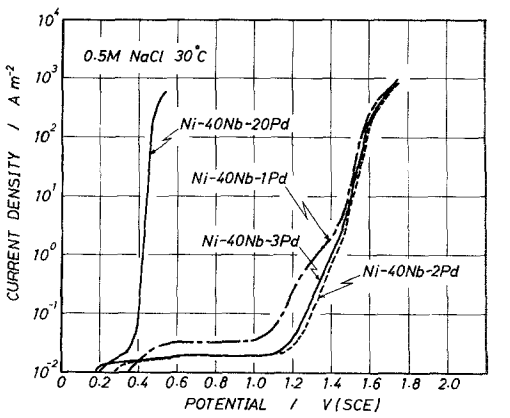

Fig. 3. Anodic polarization curves of amorphous Ni–40Nb–Pd alloys measured in 0.5 M NaCl at 30° C.

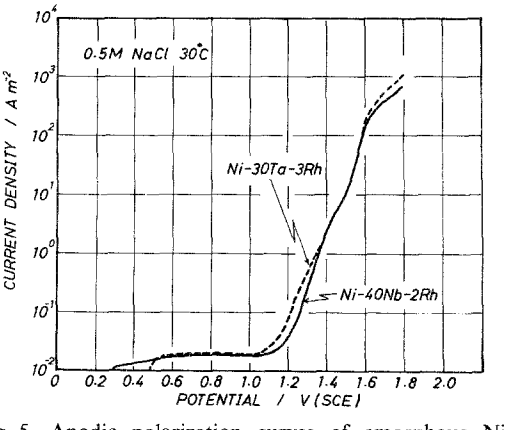

Fig. 5. Anodic polarization curves of amorphous Ni–30Ta–3Rh and Ni–40Nb–2Rh alloys measured in 0.5 M NaCl at 30° C.

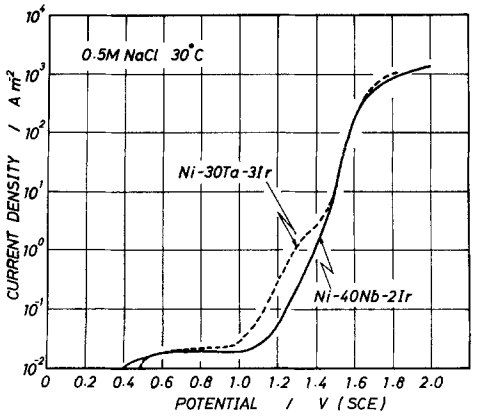

Fig. 6. Anodic polarization curves of amorphous Ni–30Ta–3Ir and Ni–40Nb–2Ir alloys measured in 0.5 M NaCl at 30° C.

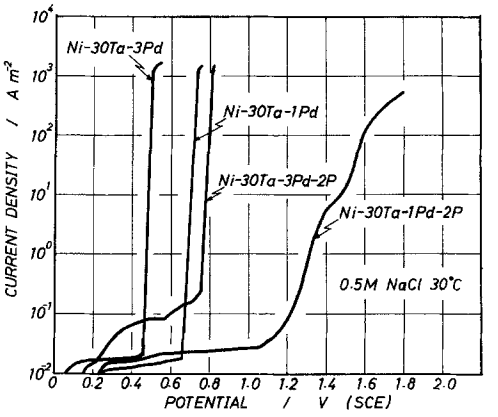

Fig. 8. Anodic polarization curves of amorphous Ni–30Ta–Pd and Ni–30Ta–Pd–2P alloys measured in 0.5 M NaCl at 30° C.

Fig. 8 exhibits a beneficial effect of phosphorus addition in the prevention of passivity breakdown. The addition of 2 at % phosphorus leads to about 300 mV ennoblement of the pitting potential for the amorphous Ni–30Ta–3Pd alloy and to immunity to pitting for the amorphous Ni–30Ta–1Pd alloy. The beneficial effect of phosphorous addition in improving the corrosion resistance and passivating ability of amorphous alloys has been previously noted [14–17], and interpreted in terms of the enhancement of formation of the passive film in which beneficial passivating ions are extraordinarily concentrated [2, 18, 19]. A combined addition of palladium and other platinum group metals such as 1 at % palladium and 0.5 at % iridium is also effective in suppressing the detrimental effect of the palladium addition.

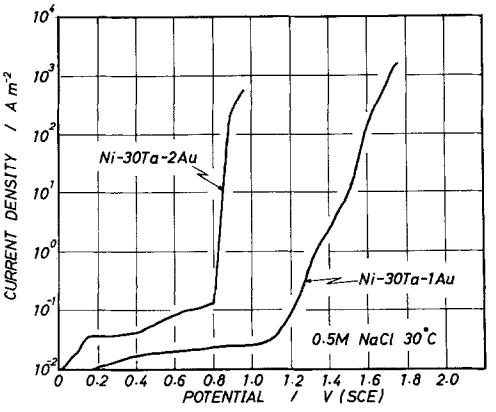

Fig. 7. Anodic polarization curves of amorphous Ni–30Ta–Au alloys measured in 0.5 M NaCl at 30° C.

3.2. *Surface-activated alloys*

Even if small amounts of platinum group metals are added to the amorphous Ni–30Ta and Ni–40Nb alloys, their electrocatalytic activity for chlorine production is too low for use as an industrial anode for the electrolysis of seawater and must be increased about four orders of magnitude. The surface activation treatment consisting of the deposition, diffusion and leaching of zinc [10–12] was not effective in increasing the electrocatalytic activity of the alloys containing valve metals such as Ni–Ti, Ni–Zr, Ni–Nb and Ni–Ta alloys because air-formed, valve metal oxide films prevented the diffusion of zinc into the amorphous alloys by heat treatment.

On the other hand, when some of these amorphous alloys were immersed in a 46% HF solution at ambient temperature their surfaces became black due to surface roughening and they showed high electrocatalytic activities for chlorine evolution. Consequently, the surface activation treatment was performed by immersion in 46% HF solution at ambient temperature for periods of a few minutes to several tens of minutes until the surface of the specimens became black. Fig. 9 shows an example depicting the effect of the surface activation treatment on the electrocatalytic activity for chlorine evolution. The activity is increased by almost four orders of magnitude and is now high enough for practical use. After the surface activation treatment the first run of the

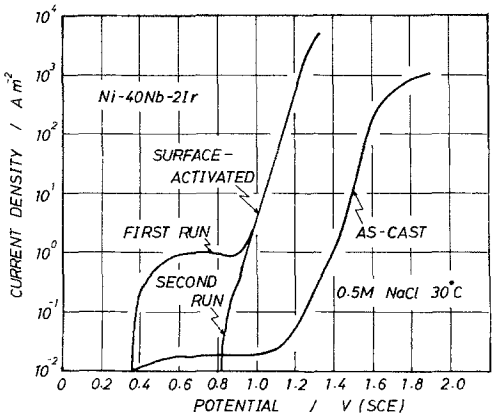

Fig. 9. Change in anodic polarization curves by surface activation treatment for the amorphous Ni–40Nb–2Ir alloy measured in 0.5 M NaCl at 30° C. The first and second runs indicate the number of measurements of the polarization curves after surface activation treatment. The solution was renewed at every measurement.

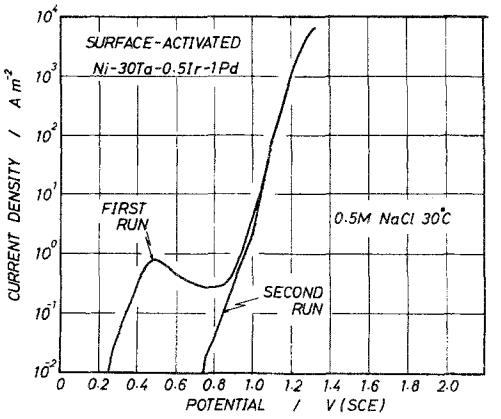

Fig. 10. Anodic polarization curves of the surface-activated amorphous Ni–30Ta–0.5Ir–1Pd alloy measured in 0.5 M NaCl at 30° C. The first and second runs indicate the number of measurements of the polarization curves after surface activation treatment. The solution was renewed at every measurement.

measurement of the polarization curve exhibits an anodic dissolution current up to about 1 A m^{-2} from about 0.35 V (versus SCE) due to dissolution of soluble elements which have not been removed by the surface activation treatment. However, once the specimen has been polarized in the potential region for chlorine production during the first run, the second run in the fresh solution shows no anodic dissolution current and gives a high open-circuit potential as well as a monotonous increase in current density with a potential rise due to chlorine evolution. This fact suggests that the anodic polarization of the surface-activated specimen in the potential region for chlorine production results in the formation of a stable passive film on which chlorine evolution takes place.

Similar polarization curves were obtained for a variety of surface-activated amorphous alloys. Another example is given in Fig. 10 which reveals that the addition of 0.5 at % iridium to the amorphous Ni–30Ta–1Pd alloy inhibits pitting corrosion induced by the addition of 1 at % palladium even after the surface activation treatment. The electrocatalytic activity of the surface-activated alloy shown in Fig. 10 is much higher than that of the surface-activated Ni–40Nb–2Ir alloy shown in Fig. 9. The amorphous alloys containing platinum group elements which did not suffer pitting corrosion by potentiodynamic polarization were able to become black by immersion in the 46% HF solution. There were, however, some alloys such as Ni–30Ta–1Au and Ni–40Nb–1Pd–2P alloys whose surface-activated layer was removed during potentiodynamic polarization.

The estimation of the corrosion rate during chlorine evolution for the surface-activated amorphous alloy specimens, whose surface-activated layer was stable during potentiodynamic polarization, was attempted by using the difference between weights measured after a 12-h polarization and after a further 24-h polarization. However, corrosion weight losses of these surface-activated amorphous alloys during the polarization for 24 h were not detected by a microbalance. Consequently, an almost complete passivation occurs by the previous polarization for 12 h, and the chlorine production takes place on the protective passive film as has been found for amorphous palladium base alloys in which chlorine evolves on their stable passive films [6].

In order to obtain a better understanding of the change in the specimen caused by the surface activation treatment, surface analysis was carried out. The analytical result is shown in Fig. 11. The left halves of the X-ray line profiles correspond to the concentrations of respective elements in the surface-activated layer, and the

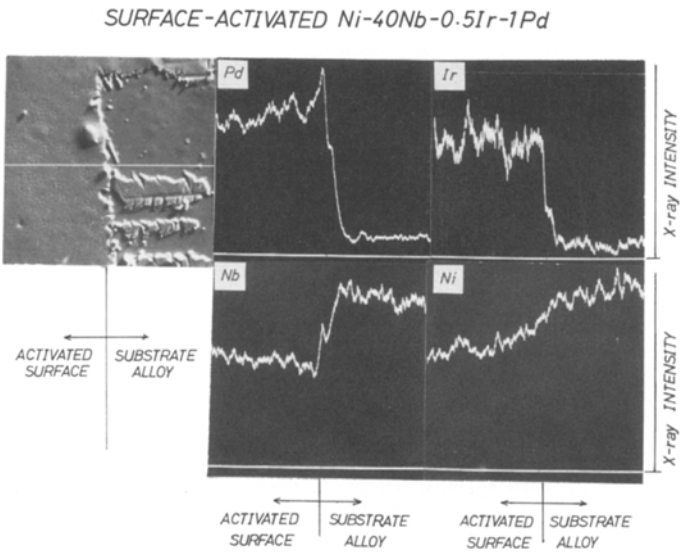

Fig. 11. Scanning electron micrograph and characteristic X-ray line profiles of the surface-activated amorphous Ni–40Nb–0.5Ir–1Pd alloy. The surface-activated layer was mechanically stripped off from the surface of the right half of the specimen and X-ray line profiles were measured along a white line seen in the scanning electron micrograph.

right halves of the X-ray line profiles to the concentrations of respective elements in the untreated amorphous alloy since the surface-activated layer was removed from the right half of the specimen surface. In the surface-activated layer the X-ray intensities of palladium and iridium are significantly higher and those of nickel and niobium are considerably lower in comparison with the untreated amorphous alloy surface. Similarly, the surface activation treatment of the amorphous tantalum-containing alloys led to preferential dissolution of nickel and tantalum. Consequently, the surface activation treatment leads to a remarkable enrichment of electrocatalytically active platinum group elements in the surface-activated layer as a result of selective dissolution of electrocatalytically less active nickel and valve metals, that is, niobium and tantalum in addition to a significant surface roughening.

Fig. 12 shows the effect of vitrification on the anodic polarization behaviour. The crystalline alloy has almost no electrocatalytic activity for chlorine evolution and a poor corrosion resistance under the electrolytic conditions. Crystalline heterogeneous alloys essentially have lower corrosion resistance and passivating ability in comparison with their amorphous counterparts of homogeneous single-phase solid solutions containing passivating elements, since a defect-free passive film cannot be formed on the heterogeneous alloys [2, 20–23]. The surface activation treatment of the crystalline alloy did not lead to the black colouration attributable to surface roughening. This fact indicates that the crystalline alloy consisting of a heterogeneous phase mixture is unsuitable for preferential dissolution of nickel and valve metals in the HF solution in order to increase the effective surface area and to accumulate beneficial platinum group elements in the surface region. When amorphous alloy specimens were immersed in the HF solution for surface activation, vigorous

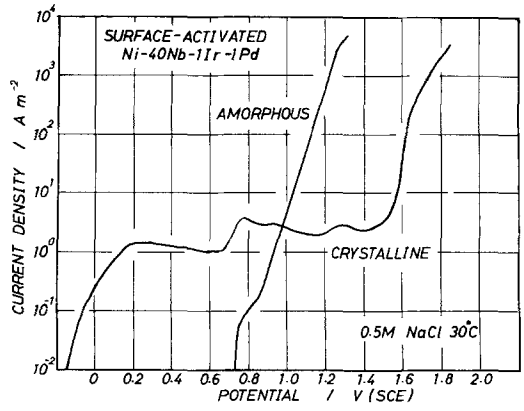

Fig. 12. Anodic polarization curves of surface-activated amorphous and crystalline Ni–40Nb–1Ir–1Pd alloys measured in 0.5 M NaCl at 30° C. Immersion of both specimens in a 46% HF solution was made for 1 min.

Table 3. Current efficiency of surface-activated amorphous alloys for galvanostatic chlorine evolution at various current densities

Alloy	*Current efficiency (%)*					
	$0.5\,kA\,m^{-2}$	$1\,kA\,m^{-2}$	$2\,kA\,m^{-2}$	$3\,kA\,m^{-2}$	$4\,kA\,m^{-2}$	$5\,kA\,m^{-2}$
Ni–30Ta–2Rh	56.3	66.2	71.4	66.9	66.9	66.0
Ni–30Ta–5Rh	58.5	66.9	71.8	66.9	66.3	63.3
Ni–40Nb–2Rh	60.3	68.6	70.0	68.8	69.4	68.2
Ni–30Ta–0.5Ir	74.2	73.0	83.8	83.8	85.6	85.0
Ni–30Ta–1Ir	68.4	76.2	84.3	84.1	85.6	85.0
Ni–30Ta–2Ir	62.7	71.5	82.6	85.0	85.2	85.2
Ni–30Ta–3Ir	70.6	76.6	82.6	85.6	85.6	84.4
Ni–40Nb–0.5Ir	50.1	62.7	74.8	74.8	76.0	75.4
Ni–40Nb–1Ir	65.1	77.2	86.9	85.6	85.6	83.2
Ni–40Nb–2Ir	63.3	74.8	85.0	84.4	84.4	84.4
Ni–30Ta–0.5Ir–1Pd	64.5	77.8	87.5	88.7	91.1	88.7
Ni–40Nb–0.5Ir–1Pd	76.0	87.5	93.5	94.1	93.5	90.5
Ni–40Nb–1Ir–1Pd	70.6	83.8	92.3	94.4	95.3	94.1

hydrogen evolution was observed. Finely and homogeneously distributed platinum group elements in amorphous alloys consisting of a single-phase solid solution is responsible for vigorous hydrogen evolution. In addition, the thermodynamically metastable nature of amorphous alloys provides high chemical reactivity unless a stable passive film is formed as in the HF solution. The high chemical reactivity and vigorous hydrogen evolution lead to preferential dissolution of electrocatalytically less active nickel and valve metals and to enrichment of electrocatalytically active platinum group elements in the surface region in addition to surface roughening. In contrast, hydrogen bubbling in the HF solution was not found for the thermodynamically stable crystalline alloys composed of multiple phases in which alloying elements are heterogeneously distributed, and hence surface activation by immersion in the HF solution for several tens of minutes was unsuccessful.

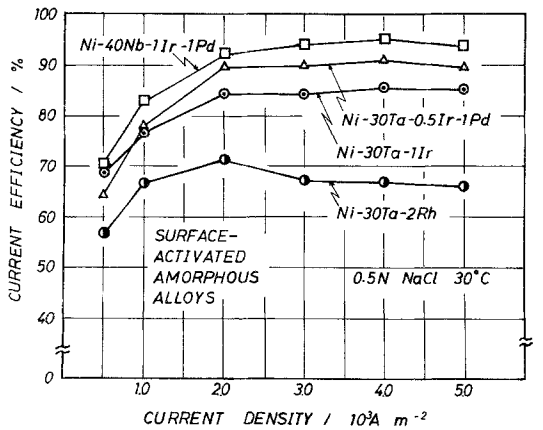

Fig. 13. The current efficiency for the chlorine evolution on surface-activated amorphous alloys for the passage of $1000\,C\,l^{-1}$.

Since anodic polarization gives rise to the evolution of both chlorine and oxygen, the current efficiency for chlorine production by galvanostatic polarization was examined by chemical analysis for chlorine and hypochlorite ion. As shown in Fig. 13 the current efficiency of surface-activated amorphous alloys for chlorine production is almost independent of the current density at $2000\,A\,m^{-2}$ or higher current densities, and depends on the alloy composition. Table 3 shows the change in the current efficiency with additive platinum group elements. When rhodium is added as an electrocatalytically active element, the current efficiency for chlorine evolution is not relatively high, ranging from 66 to 70%. The iridium-containing alloys have higher current efficiencies, ranging from 75 to 85%. The maximum current efficiency of the Pt–Ir/Ti electrode, which has been known to have the highest activity among currently used electrodes for production of sodium hypochlorite by the electrolysis of seawater, is about 80% in the 0.5 M NaCl solution at 30° C [9]. Accordingly, most of the surface-activated amorphous iridium-containing alloys possess

higher electrocatalytic activities for chlorine production in comparison with the currently used, most active Pt–Ir/Ti electrode. The palladium-containing alloys have further higher electrocatalytic activities for chlorine evolution and their current efficiency reaches 95%.

Therefore, current efficiency for chlorine production is dependent upon the additive platinum group elements; palladium is most effective, iridium is the second and the addition of rhodium alone is also effective but results in the current efficiency of about 70% for chlorine evolution. This order of additive platinum group elements for chlorine production in 0.5 M NaCl solution at ambient temperature is the same as that found in a hot concentrated sodium chloride solution such as 4 M NaCl at 80° C [6, 24].

References

[1] M. Naka, K. Hashimoto and T. Masumoto, *J. Japan Inst. Metals* **38** (1974) 835.

[2] K. Hashimoto, 'Rapidly Quenched Metals', Proceedings of 5th International Conference on Rapidly Quenched Metals (edited by S. Steeb and H. Warlimont), Elsevier Science Publishers, Amsterdam (1985) Vol. II, p. 1449, p. 1109.

[3] M. Hara, K. Hashimoto and T. Masumoto, *Electrochim. Acta* **25** (1980) 1091.

[4] *Idem, J. Appl. Electrochem.* **13** (1983) 295.

[5] *Idem, J. Non-cryst. Solids* **54** (1985) 85.

[6] M. Hara, K. Asami, K. Hashimoto and T. Masumoto, *Denki Kagaku* **53** (1985) 785.

[7] *Idem, Electrochim. Acta* **31** (1986) 481.

[8] N. Kumagai, A. Kawashima, K. Asami and K. Hashimoto, 'Rapidly Quenched Metals', Proceedings of 5th International Conference on Rapidly Quenched Metals (edited by S. Steeb and H. Warlimont), Elsevier Science Publishers, Amsterdam (1985) Vol. II, p. 1795.

[9] *Idem, J. Appl. Electrochem.* **16** (1986) 565.

[10] A. Kawashima and K. Hashimoto, 'Rapidly Quenched Metals', Proceedings of 4th International Conference on Rapidly Quenched Metals (edited by T. Masumoto and K. Suzuki), The Japan Institute of Metals, Sendai (1982) Vol. II, p. 1427.

[11] *Idem*, Sci. Rep. Res. Inst. Tohoku University A-31 (1983) 174.

[12] N. Kumagai, K. Asami and K. Hashimoto, *J. Non-cryst. Solids* **87** (1986) 123.

[13] N. Kumagai, K. Asami, A. Kawashima and K. Hashimoto, *J. Electrochem. Soc.* **133** (1986) 1876.

[14] M. Naka, K. Hashimoto and T. Masumoto, *J. Non-cryst. Solids* **30** (1978) 29.

[15] M. Naka, K. Asami, K. Hashimoto and T. Masumoto, 'Titanium '80', Proceedings of 4th International Conference on Titanium (edited by H. Kimura and O. Izumi), The Metallurgical Society of AIME, Warrendale, PA (1981) Vol. 4, p. 2677.

[16] T. D. Burleigh and R. M. Latanision, 'Passivity of Metals and Semiconductors', Proceedings of 5th International Symposium on Passivity (edited by M. Froment), Elsevier Science Publishers, Amsterdam (1983) p. 321.

[17] K. Shimamura, A. Kawashima, K. Asami and K. Hashimoto, Sci. Rep. Res. Inst. Tohoku University, A-33 (1986).

[18] K. Hashimoto, M. Naka, K. Asami and T. Masumoto, *Corros. Eng.* (*Boshoku Gijutsu*) **27** (1978) 279.

[19] K. Hashimoto, K. Asami, M. Naka and T. Masumoto, *Corros. Sci.* **19** (1979) 857.

[20] K. Hashimoto, K. Osada, T. Masumoto and S. Shimodaira, *ibid.* **16** (1976) 71.

[21] K. Hashimoto and K. Asami, 'Passivity of Metals', (edited by R. P. Frankenthal and J. Kruger), The Corrosion Monograph Series, The Electrochemical Society, Princeton, NJ (1978) p. 749.

[22] K. Hashimoto, 'Passivity of Metals and Semiconductors', Proceedings of 5th International Symposium on Passivity (edited by M. Froment), Elsevier Science Publishers, Amsterdam (1983) p. 235.

[23] M. Hara, K. Asami, K. Hashimoto and T. Masumoto, *Corros. Eng.* (*Boshoku Gijutsu*) **32** (1983) 363.

[24] *Idem, Electrochim Acta* **28** (1983) 1073.